Superconducting Niobium Thin Film Slow-Wave Structures

J. J. Bautista and S. M. Petty
Radio Frequency and Microwave Subsystem Section
L. H. Allen, M. R. Beasley and R. H. Hammond
Stanford University

A superconducting comb structure as a slow-wave element in a traveling-wave maser will significantly improve maser noise temperature and gain by reducing the insertion loss. This article presents the results of the insertion loss measurements of superconducting niobium slow-wave structures subjected to maser operating conditions at X-Band frequencies.

I. Introduction

In a traveling wave maser the principle function of a slow-wave structure is to increase the interaction time of the received signal with the maser material in order to maximize the gain per unit length. The increased gain per unit length will, unfortunately, be accompanied by a proportional increase in ohmic losses per unit length (Refs. 1, 2). The proportionality constant is determined by the material's microwave properties and its temperature.

At low temperatures and high frequencies it is well known that the microwave surface resistance for normal metals is severely limited by the so called "anomalous skin effect" (Ref. 3). For sufficiently high temperatures (depending on the material) and at microwave frequencies the conduction electron mean free path is short compared to the spatial variation of the electromagnetic field. For this classical limit the field is regarded as constant and Ohm's law is applied to derive the skin depth which is found to be inversely proportional to the square root of the electrical conductivity. However, at low temperatures the mean free path exceeds both the spatial variation of the field and the classical skin depth. In this limit the surface resistance becomes independent of the conductivity and temperature, since the only electrons that can contribute to the conductivity are those that remain within the skin depth between collisions (Ref. 4). In fact, the limiting surface resistance of a normal metal like copper at low temperatures (below 50 K) is approximately one-fourth to one-fifth the room temperature value (Ref. 5).

Although the microwave surface resistance of a superconductor is not zero below the critical temperature (T_c), it can be several orders of magnitude less than the best normal conductor. In fact, for $T < 0.5T_c$ the surface resistance can be approximated by the following expression (Ref. 6)

$$R_s \sim f^2/T \exp(-\Delta/kT) \qquad (1)$$

where f = frequency, T = temperature, k = Boltzman constant and 2Δ = superconducting energy gap.

This finite surface resistance can be understood by recalling that electrons in the superconducting state are bound into

electron pairs by an interaction involving the lattice vibrations of the metal. The binding energy (2Δ) is $2\Delta(0)$ at $T = 0$ K and approaches zero as T approaches T_c. At $T = 0$ K all of the electrons are bound pairs. However, for finite temperatures the thermal energy present will excite and break some of the electron pairs. In this case the number of electrons excited across the gap is proportional to the Fermi-Dirac distribution function which for $T < T_c$ can be approximated by

$$\exp - (\Delta/kT) \qquad (2)$$

Thus, photons (having a frequency $f < 2\Delta/h$) interacting with these electrons will result in the absorption of energy. Power dissipation occurs when these electrons relax to a lower energy (Ref. 7).

II. Slow-Wave Structure Preparation

The sapphire substrates (length = 3.7 in., width = 0.22 in. and thickness = 0.030 in.) were supplied by INSACO (Quaker Town, Penn.) with one side epi-finished and the c-axis parallel to the longest dimension. Before the deposition the substrates were carefully cleaned with H_2SO_4 and rinsed with deionized water and acetone.

The niobium thin films studied were deposited utilizing two different techniques – magnetron sputtering (Ref. 8) and e-beam evaporation (Ref. 9). The sputtering was performed with the substrate held at room temperature while the evaporation was done with the substrate held at approximately 700°C. Both processes yielded film thicknesses (estimated from the deposition rates) of approximately 1 μm.

The slow-wave pattern which consists of adjacently coupled, half-wavelength resonators (Ref. 10) was produced using conventional photolithographic techniques. A positive photoresist (Shipley 1470) was used to develop the pattern and the excess niobium was removed using a plasma assisted etching technique (Ref. 11).

Pictured in Figs. 1 and 2 are the best samples obtained from the two deposition techniques. Visual inspection of the samples indicates that the better set was produced with the e-beam evaporation technique. The sputtered samples appear blistered and not to have adhered as well to the substrate as the e-beam samples. Unfortunately, this is a consequence of the cooler substrate temperature.

III. Insertion Loss Measurements

A. Microwave Circuit Structure

The microwave circuit of interest (slow-wave structure) is basically a set of 44 unbalanced, stripline resonators, approximately one-half wavelength long at X-band which are adjacently coupled to one another. The niobium thin film resonators are sandwiched between two dielectric substrates – a 40 mil thick ruby bar on one side and 30 mil sapphire and 68 mil alumina bar on the other. The ground planes are defined by the inner copper channel walls of the assembly pictured in Fig. 3. It should be noted that the cross-sectional dimensions of the copper are chosen so that the TE_{20} mode of the pump frequencies (19 and 24 GHz) is supported. In addition, the resonator strip and dielectric dimensions are chosen so that the characteristic impedance of the resonators is approximately 50 ohms. Coupling into and out of the slow-wave structure is achieved with identical coaxial to stripline (copper) transitions whose center conductor is out of the plane of the slow-wave structure but parallel to first element and spaced a distance equal to spacing between adjacent elements. (For a more detailed description of this structure please see Ref. 10.)

B. Cryogenic Apparatus

A sketch of the cryogenic apparatus utilized for the insertion loss measurements is shown in Fig. 4. It consists of two comb structures connected in series for increased measurement sensitivity. The measurements obtained at low temperatures were performed with the apparatus immersed in liquid helium maintained at 4.5 K.

The applied dc magnetic field was supplied by an external electromagnet. The magnet and cryogenic apparatus were positioned such that the direction of magnetic field could be rotated through 180° with respect to a normal through the film-substrate interface.

C. Measurement Setup

A swept measurement technique was utilized for performing the insertion loss measurements. To minimize heat leaks from room temperature to the helium bath stainless steel coaxial lines were used for the signal input and output. Figure 5 contains a block diagram showing the measurement set up.

IV. Results

Prior to commencing the low temperature measurements the insertion loss for the two combs was observed using 5 mW of signal power as the samples cooled. It is interesting to note that the insertion loss of the niobium combs in the normal state was observed to change from 70 dB at 300 K to approximately 8 dB at 10 K (see Fig. 6) while comparable copper combs are known to change only from 10 dB to 4 dB over the same temperature range (R. B. Quinn, private communication).

This significant difference in temperature behavior can be understood by noting that at 8.0 GHz the classical to anomalous "transition" of the surface resistance of copper occurs near 50 K while for Nb this occurs at approximately 13 K (Ref. 12).

A. Signal and Pump Power Level Effects

The microwave performance of a superconductor can be seriously degraded when driven into the normal state. There are two possible mechanisms which can cause this. In one case the peak rf magnetic field can exceed the thermodynamic critical field H_c (H_c = 1900 gauss at T = 0 K for niobium). Inadequate heat dissipation can account for the other mechanism resulting in thermal runaway.

For the second case the rf ohmic losses are not readily dissipated because of a low thermal conductivity and/or poor thermal heat sinking. The resulting increase in temperature rapidly drives the superconductor above its critical temperature T_c (T_c = 9.2 K for niobium). This will occur before the peak rf field exceeds B_c (Ref. 6, 7, 13).

For maser or low power applications heat dissipation is the more important concern. This problem was clearly evidenced when the sputtered niobium combs were first tested in vacuum with the copper ground planes thermally anchored to 4.5 K. For these tests, only modest levels of signal and pump power (approximately 50 mW) were required to significantly degrade the insertion loss.

This problem was alleviated when the combs were measured while immersed in liquid helium. In fact, the insertion loss was found to be nearly independent of signal power up to 800 mW and pump power up to 250 mW (see Fig. 7).

B. Magnetic Field Effects

In order to demonstrate feasibility for use in an X-band maser these structures must remain superconducting in the presence of a dc magnetic field up to 5.5 kgauss. For this part of the study the insertion loss was measured at the passband as a function of the applied dc magnetic field from 0 to 10 kgauss for two orientations (parallel and perpendicular) to the direction of the microwave surface currents.

Figure 8 contains a sample of the measured results obtained for the evaporated combs with the magnetic field in the perpendicular direction. Similar results were obtained for the sputtered combs. The results demonstrated that the field readily penetrates both types of films for this orientation.

Figure 9 contains a sample of results obtained for the evaporated combs with the field in the parallel direction. Similar results were obtained for the sputtered combs. For this orientation it was noted that the measured insertion loss is apparently independent of the magnetic field up to a particular field value. For the sputtered comb this field value was near 5.0 kgauss while for the evaporated film this value was approximately 3.0 kgauss.

Since the insertion loss was found to be sensitive to the magnitude and direction of the magnetic field, the perpendicular position was found (within ±0.5°) by maximizing the loss while rotating the field. The parallel position was then defined by a 90° rotation relative to the perpendicular position.

It should be mentioned before proceeding that these measurements were performed with 5 mW or less of signal power. Furthermore, the samples were tested for hysteretic effects, but none were found within the limits of these measurements.

V. Results and Discussion

A. Insertion Loss

The theoretical insertion loss in dB of a microwave (Tchebyscheff) filter at midband is given by the following expression (Ref. 14)

$$L_0\,(\text{dB}) = 4.343\,\frac{f_0}{\Delta f}\,\frac{1}{Q_u}\sum_{k=1}^{n} g_k \qquad (3)$$

where f_0 is the filter center frequency, Δf is the equal ripple band width, Q_u is the unloaded resonator Q, and g_k are the low-pass prototype filter element values. Now, for a microstrip structure the total loss is the sum of the dielectric, ohmic and radiative losses. That is (Ref. 15, 16),

$$Q_u^{-1} = Q^{-1}\,(\text{dielectric}) + Q^{-1}\,(\text{ohmic}) + Q^{-1}\,(\text{radiative}) \qquad (4)$$

A few simplifying approximations are necessary in order to compare the measured with the expected insertion loss results. Since the reported Q values of sapphire vary from 10^5 to 10^9 (Ref. 17) and since Q (radiative) is essentially infinite for resonators enclosed in a waveguide below cut off, then it is reasonable to assume that $Q_u \simeq Q$ (ohmic). Furthermore, for the special case of a 50 Ω halfwave length resonator open at both ends (Ref. 18)

$$Q_u \simeq 800\,(h/\lambda)\,R_s^{-1} \qquad (5)$$

where h = dielectric thickness, λ = free space wavelength and R_s = the surface resistance of the conducting strip.

In Eq. (3) the g_k's depend on the in-band ripple. Based on the observed return loss and the inband response (see Fig. 10) the summation of the g_k's for $n = 44$ is approximately 100 and $f_0/\Delta f = 6.5$. In addition, in Eq. (5) $h = 0.040$ in. and $\lambda = 1.5$ in. Substituting these values into Eq. (3) yields that

$$L_0\,(\text{dB}) \simeq 145\,R_s, \text{dB} \tag{6}$$

Table 1 contains a comparison of the measured insertion loss values and the expected values using the above approximations. With the exception of the last row, the data are within at least an order of magnitude of the expected values.

Although the agreement (as should have been expected) is poor, it is still instructive to examine the reason for the large discrepancy between the values in the last row which differ by nearly two orders of magnitude. Equation (5) assumes that the strip and ground plane have the same value for the surface resistance. Furthermore, it is generally assumed for microstrip structures that most of the ohmic loss occurs at the strip conductor and not the ground plane (Ref. 15). In this experiment the ground plane is constructed of copper so that the loss is thus dominated by the ground plane when the strip becomes superconducting.

B. Magnetic Field Effects

Although it would have been desirable to use a superconducting ground plane, the most important question to answer for maser applications is whether the slow-wave structure will retain its low loss property at the operating magnetic field values. This question can be answered without the need of a superconducting ground plane.

In order to clearly demonstrate this Figs. 11 and 12 show the normalized insertion loss as a function of applied magnetic field for both evaporated and sputtered films, respectively. Here the normalized insertion loss is defined as the ratio of the insertion loss in the superconducting state to the insertion loss in the normal state.

To first order for a quasi-TEM mode it can be assumed that the microwave currents are primarily along the direction of the half-wavelength resonator (Ref. 19). Figures 11 and 12 thus display the normalized insertion loss for the field perpendicular and parallel to both the microwave surface currents and the film substrate interface.

With the field in the perpendicular direction both the sputtered and evaporated samples show an almost linear dependence on the magnitude of the applied magnetic field until the sample reaches the normal state for a critical magnetic field (H_{c2}). Here the critical magnetic field value for the evaporated samples is 5.0 kgauss while for the sputtered samples it is 9.0 kgauss.

For the case where the magnetic field is parallel to the microwave currents the normalized insertion loss is independent of the field up to a certain value. This field value occurs at 3.0 kgauss for evaporated samples while for the sputtered samples it occurs at 5.0 kgauss. As the field is increased further to a higher critical field (H_{c3}) both samples will eventually reach the normal state. These field values are beyond the limits of the magnet used, thus are not included in Figs. 11 and 12.

The observed field dependence of the normalized insertion loss can be qualitatively understood by recalling some of the properties of a type-II superconductor. For a type-II superconductor like Nb the Meissner state (the exclusion of flux from the interior of the superconductor) exists for field values below the first critical field value H_{c1}. Above H_{c1} and below H_{c2} the mixed state is present. In this field range magnetic flux penetrates the sample in the form of quantized flux lines and the superconductor exhibits a two dimensional structure that consists of normal regions through which flux penetrates surrounded by superconducting regions (Refs. 20, 21).

It is the interaction of the microwave current with the flux lines through the Lorentz force that results in power dissipation. That is, the force per unit length of flux line is given by

$$\vec{f}_L = \vec{j} \times \vec{\Phi}_0 \tag{7}$$

where $\vec{j}$ is the microwave current density and $\Phi_0 = hc/2e = 2.07 \times 10^{-7}$ gauss-cm^2 is a quantum of flux. At microwave frequencies the oscillatory motion of the flux lines occurs through a medium that is regarded as viscous resulting in power loss (Ref. 22). Thus, when the current and field are perpendicular and $H > H_{c1}$ the loss is expected to increase linearly with the field up to H_{c2}. Now, for the case where the field and current are parallel Eq. (7) is zero and the loss is expected to be independent of flux-flow losses as H_{c2} is approached (Ref. 22).

Above H_{c2} for the parallel direction the sample is in the sheath state where the outside surface remains superconducting and the inner portion is in the normal state (Refs. 20, 21). The thickness of the sheath is of the order of the coherence length ($\xi \sim 400$ Å) which is comparable to λ_L (the London penetration depth). As the field is increased the sheath thickness decreases resulting in an increased loss up until H_{c3} is reached where the sample becomes normal (Ref. 23).

The observed quantitative difference in H_{c2} and H_{c3} for the sputtered and evaporated samples is related to the manner in which they were prepared. The parameter that determines H_{c2} and H_{c3} is the coherence length ξ which is the range of coherence of the superconducting phase. The critical fields are given by the following expressions (Ref. 22):

$$H_{c2}(T) = \frac{1}{2\pi} \Phi_0/\xi^2(T)$$

and

$$H_{c3}(T) = 1.695\, H_{c2}(T) \tag{9}$$

where

$$\frac{1}{\xi} = \frac{1}{\xi_0} + \frac{1}{\alpha \ell} \tag{10}$$

and where ξ_0 = intrinsic coherence length at $T = 0$ K, ℓ = the electron mean free path and α is an adjustable parameter. Since it is known that annealing thin film Nb samples increases the electron mean free path, it is expected that the evaporated samples will have a longer mean free path. Thus Eqs. (8), (9) and (10) imply that the critical fields are expected to be lower for the evaporated films which was verified by the measurements.

VI. Remarks and Conclusion

It has been demonstrated that thin film, type-II superconducting materials are feasible for use as slow-wave comb structures in a ruby maser. Although it does not appear that Nb is useful at X-band frequencies, the results do indicate that Nb can be used at S-band frequencies where the applied magnetic fields are less than 3.0 kgauss.

For frequencies at X-band and higher Nb_3Sn should be a suitable candidate. Its surface resistance at X-band and helium temperatures has displayed values less than 1/30 of the values for the Nb samples tested. Furthermore, Nb_3Sn has an H_{c2} of approximately 200 kgauss (nearly 100 times the value for Nb).

Although there are other possible slow-wave structures that could have been tested, these results and previous measurements (Ref. 22) dictate that the structures must be thin along the direction of the field and the microwave currents must also be parallel to this direction. For example, the microwave Pb meander line evaluated by Gandolfo *et al.* (Ref. 23) would have the thin dimension parallel to the field. However, portions of the line would have segments where the microwave currents are perpendicular to the field. Kim (Ref. 22) has observed that the surface resistance (for films having this orientation) is intermediate between the values for the perpendicular and parallel direction. Thus a half-wave comb structure is clearly the optimal slow-wave circuit for these applications.

The noise temperature of a traveling wave maser having a high gain ($G \gg 1$) is given by (Refs. 1, 24, 25)

$$T_m = T_0 \frac{\rho + \beta}{1 - \beta} \tag{11}$$

and the net gain by

$$G(\text{dB}) = \text{Electronic Gain (dB)} - \text{Forward Loss (dB)} \tag{12}$$

where ρ = (Inversion Ratio)$^{-1}$, β = Forward Loss (dB)/Electronic Gain (dB) and T_0 = Bath Temperature. For comparison Table 2 contains the expected T_m and G(dB) for several different metals utilizing the same slow-wave structure pattern (Ref. 10). The values assumed for the Inversion Ratio and the Electronic Gain are typical and nearly ideal values measured for the Block II-A X-band traveling wave masers (D. L. Trowbridge, private communication). It should be mentioned that the best estimate of the isolator contribution to the Forward Loss is from 1 to 2 dB. However, this loss can in principle be further reduced (Ref. 26).

In conclusion, it is noted that Nb_3Sn structures could in principle reduce the noise temperature of existing Block II-A masers by approximately 50% and increase the net gain by 20%. Evidently, the net gain could be further improved by increasing the slowing without significantly increasing the noise temperature. An alternate and possibly more desirable approach would be to widen the bandwidth while keeping the gain and noise temperature constant. Furthermore, Nb_3Sn would be of greater benefit at higher frequencies where dissipative loss is often a more serious problem.

References

1. Siegman, A. E., *Microwave Solid State Masers* (McGraw-Hill Book Company, New York, 1964).
2. Ishii, T. K., *Maser and Laser Engineering* (Robert E. Krieger Publishing Company, New York, 1980).
3. Pippard, A. B., Proc. Roy. Soc. *A191*, 385 (1947).
4. Reuter, G. E. H., and Sondheimer, E. H., Proc. Roy. Soc. *A195*, 336 (1948).
5. Bernard, J., El Minyawi, N. H., and Viet, N. T., Revue de Physique Appliquée *13*, 483 (1978).
6. Septier, A., and Viet, N. T., J. of Phy. E. Sci. Inst. *10*, 1193 (1977).
7. Turneaure, J. P., Proc. 8th Int. Conf. on High Energy Accelerators *51* (Geneva, Switzerland, 1971).
8. Barbee, T. W., and Keith, D. L., "Synthesis of Metastable Materials," Conf. Proc. of the Metal. Soc. of AIME, Pittsburg, 1980.
9. Hammond, R. H., IEEE Trans. Magn. *MAG-11*, 201 (1975).
10. Clauss, R. C., Quinn, R. B., Petty, S. M., and Trowbridge, D. L., "Maser Amplifier Slow-Wave Structure," JPL Case No. 15211 (NASA NPO-15, 211-1).
11. Melliar-Smith, C. M., and Mogab, C. J., in *Thin Film Processes*, Vossen, J. L. and Kern, W., ed. (Academic Press, New York, 1978).
12. Ratcke, J. E., *The Transient Analysis of Coaxial Cables at Low Temperatures Considering Anomalous and Classical Skin Effects with the Inclusion of Electron Relaxation Phenomena*, Ph.D. Thesis, University of Kansas (1969).
13. Kuntze, M., Proc. 9th Inst. Conf. on High Energy Accelerators, 115 (Stanford, 1974).
14. Matthaei, G. L., Young L. and Jones, E. M. T., *Microwave Filters, Impedance-Matching Networks, and Coupling Structures* (Artech House Books, Dedham, Mass., 1980).
15. Pucel, R. A., Masse, D. J., and Hartwig, C. P., IEEE Trans. on Theory and Techniques *MTT-16*, 342 (1968).
16. Denlinger, E. J., IEEE Trans. on Theory and Techniques *MTT-17*, 235 (1969).
17. Braginsky, V. B. and Panov, V. I., IEEE Trans. on Mag. *MAG-15*, 30 (1979).
18. Davidheiser, R. A., AIP Conf. Proc. *44*, Future Trends in Superconducting Electronics, AIP, 219 (1978).
19. Denlinger, E. J., IEEE Trans. on Microwave Theory and Techniques *MTT-19*, 30 (1971).
20. Berlincourt, T. G., in *Superconductivity in Science and Technology*, Cohen, M. H., ed (University of Chicago Press, Chicago, 1968).
21. Rose Innes, A. C., and Rhoderick, E. H., *Introduction to Superconductivity* (Pergamon Press, London, 1969).
22. Kim, S. H., *Microwave Surface Impedance of Superconductors*, Ph.D. Thesis, Wayne State University (1975).

23. Gandolfo, D. A., Boornard, A., and Morris, L. C., J. of App. Phys. *39*, 2657 (1968).

24. Higa, W. H., IEEE Trans. on Microwave Theory and Techniques *MTT-12*, 2 (1964).

25. Clauss, R. C., JPL Space Programs Summary 37-45, *Vol. III*, 40 (April, 1967).

26. Clauss, R. C., "Resonant Isolator for Maser Amplifier," JPL Case No. 15201 (NASA NPO-15201).

Table 1. Insertion loss at mid-band for X-band comb

Slow-wave structure	Temp, K	R_s, Ω	Calculated I.L.[a], dB	Measured I.L.[a], dB
Cu	300	2.2×10^{-2}	3.2	5.0
Cu	4.5	4.0×10^{-3}	0.6	2.0
Nb-sputtered	300	–	–	35.0
Nb-evaporated normal state	300	–	–	30.0
Nb-sputtered	4.5	–	–	5.0
Nb-evaporated s.c. state	4.5	1.0×10^{-3}	1.5	3.0
Nb-sputtered	4.5	–	–	1.0
Nb-evaporated	4.5	2.0×10^{-4}	0.03	1.2
Nb_3Sn-evaporated	4.3	3.3×10^{-5}	0.005	–

[a]I.L. - Insertion loss

Table 2. T_0 = 4.5 K

Slow-wave structure	T_m	G(dB)	β	ρ
Cu	2.9[c]	44	10/54	1/3.0
Nb[a]	2.0	50	4.0/54	1/3.0
Nb[b]	1.5	54	0.12/54	1/3.0
Nb_3Sn[b]	1.5	54	0.03/54	1/3.0

[a]Superconducting resonators with Cu ground plane
[b]Superconducting resonators with superconducting ground plane
[c]Typical measured value is 3.5 K

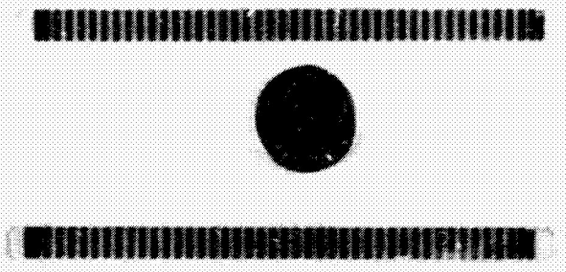

Fig. 1. Sputtered niobium, X-band slow-wave structures

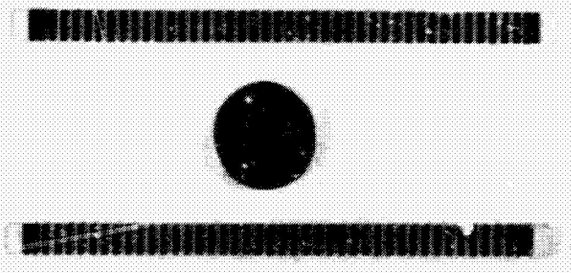

Fig. 2. Electron beam evaporated X-band slow-wave structures

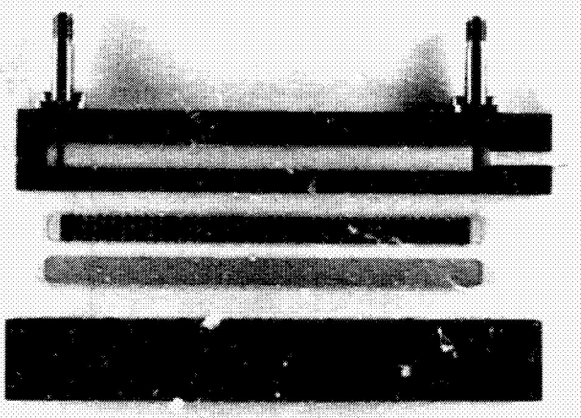

Fig. 3. Disassembled microwave circuit structure

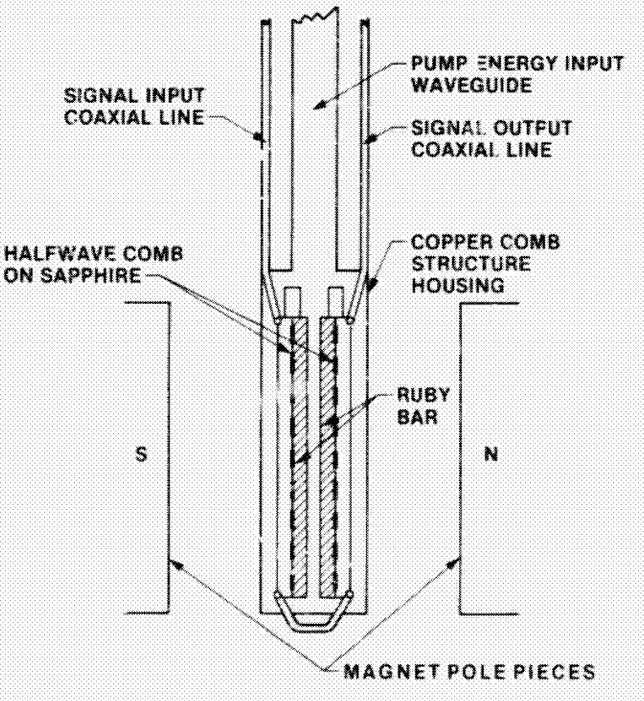

Fig. 4. Sketch of the cryogenic apparatus

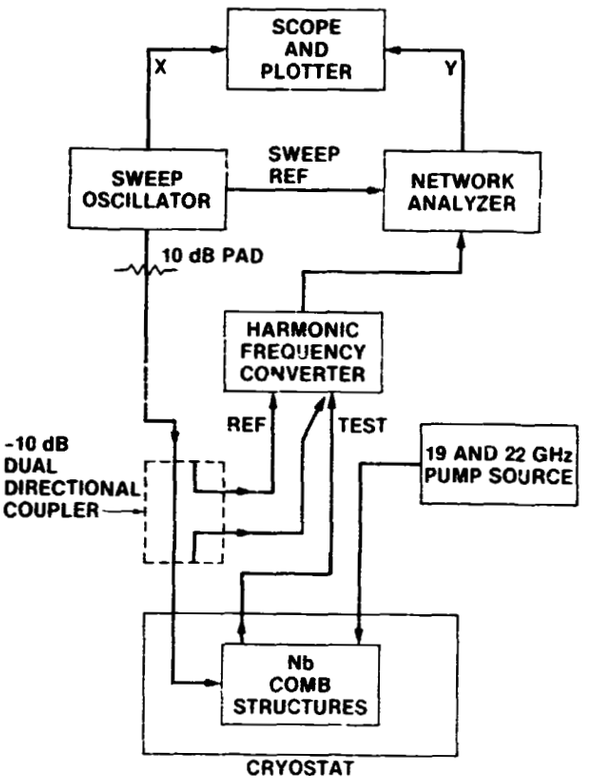

Fig. 5. Block diagram of the sweep measurement set-up

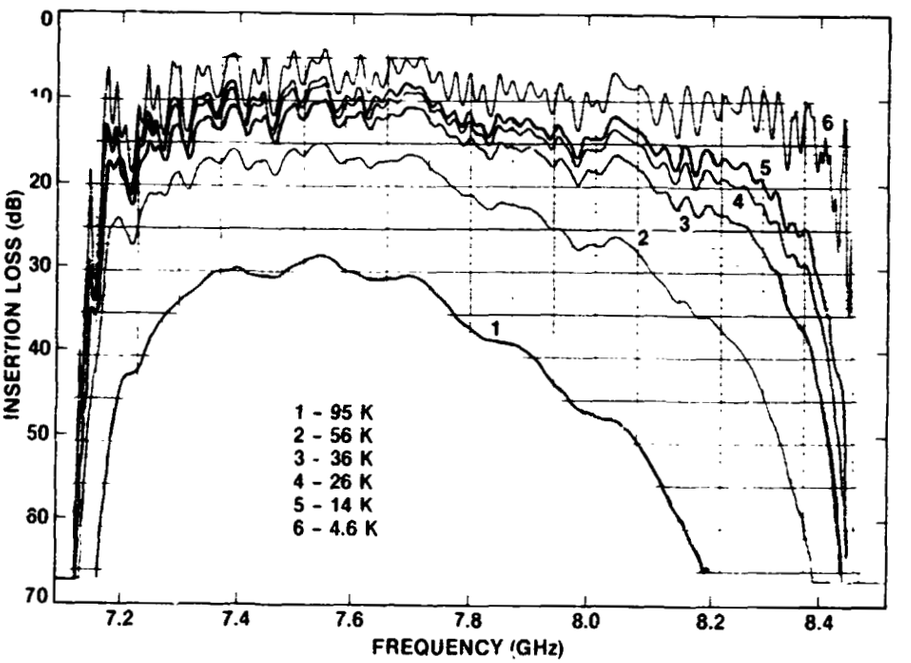

Fig. 6. Insertion loss of evaporated Nb combs at several temperatures

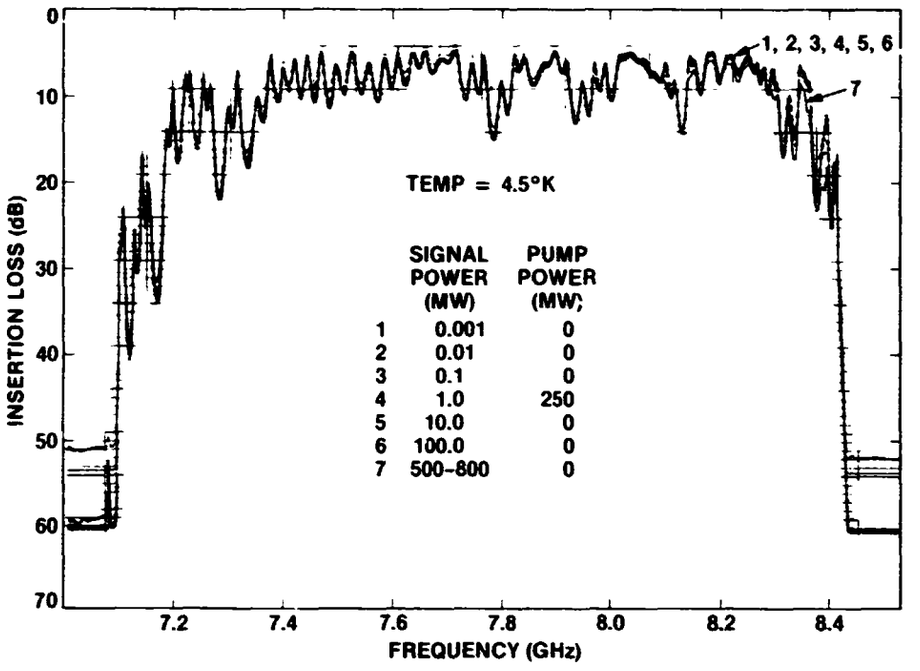

Fig. 7. The insertion loss at various values of signal and pump power for the sputtered Nb combs

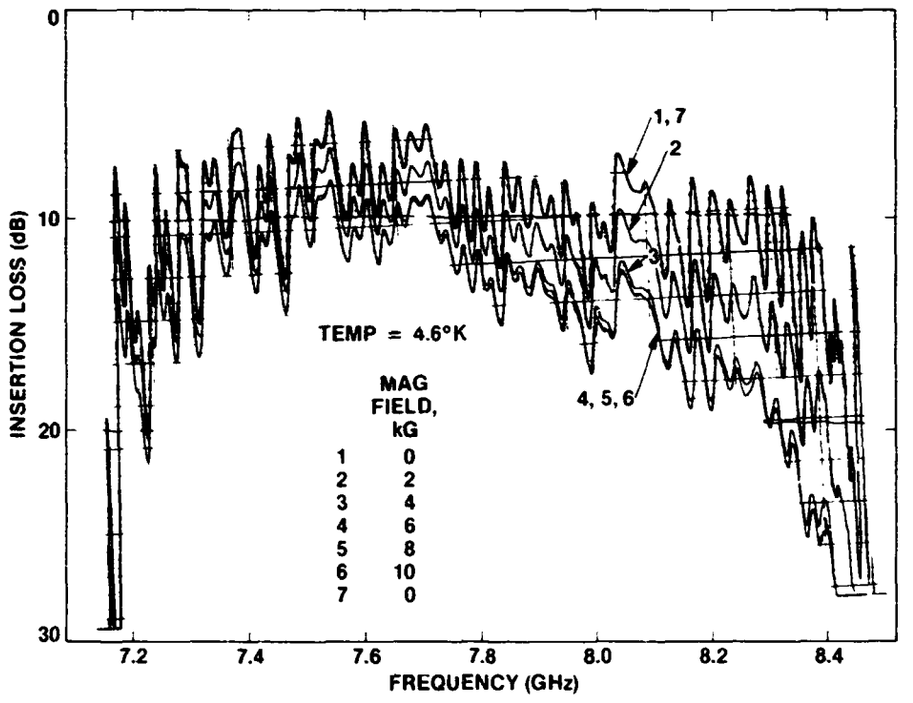

Fig. 8. Uncorrected insertion loss for several values of applied magnetic field perpendicular to the evaporated structures

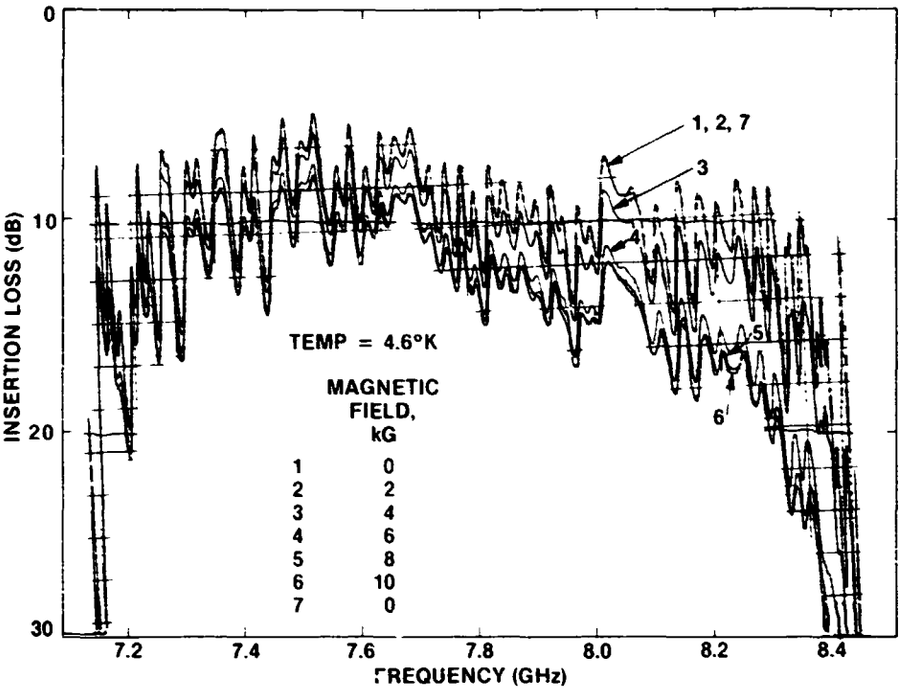

Fig. 9. Uncorrected insertion loss for several values of applied magnetic field parallel to the evaporated structures

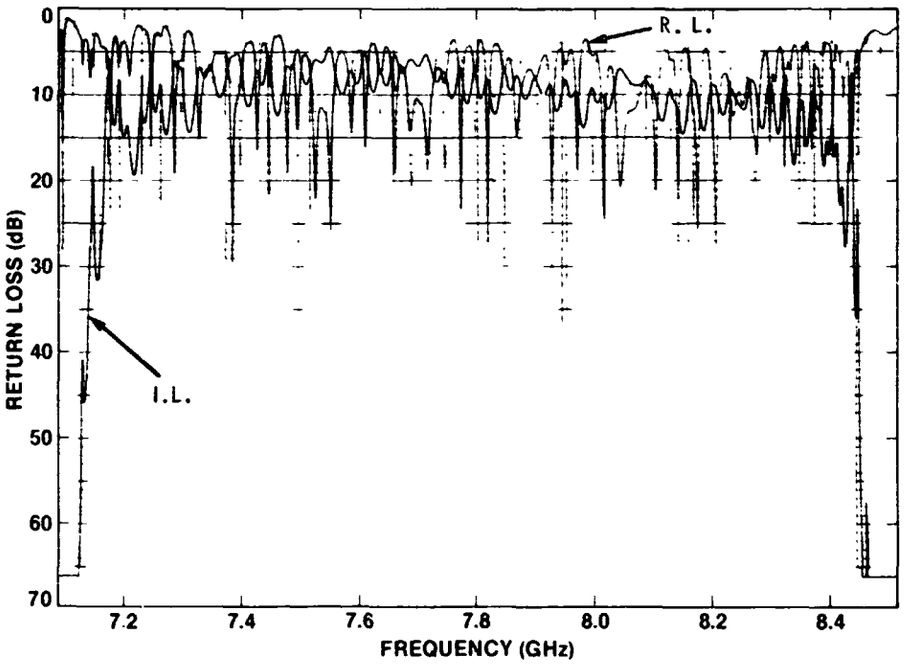

Fig. 10. The uncorrected return loss and insertion loss of the evaporated combs at 4.6 K

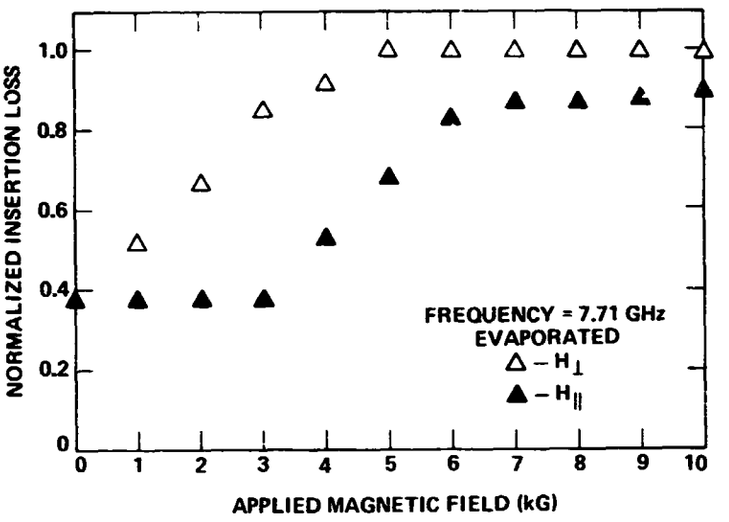

Fig. 11. The normalized insertion loss of the evaporated combs as a function of applied magnetic field

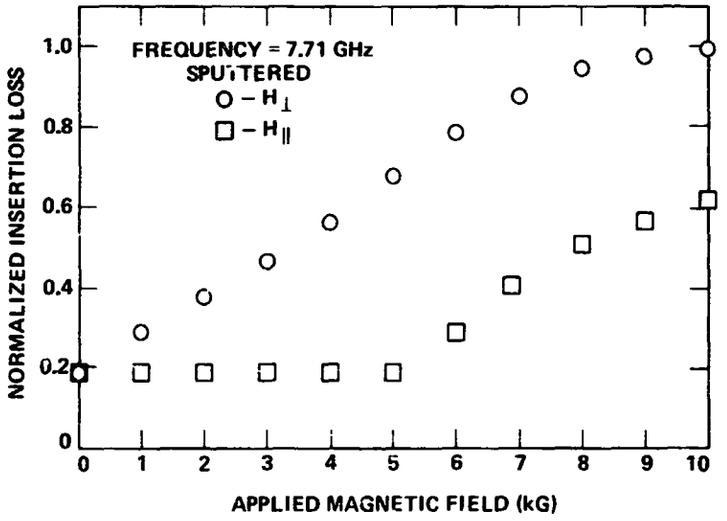

Fig. 12. The normalized insertion loss of the sputtered combs as a function of applied magnetic field